ELSEVIER

International Journal of Mass Spectrometry 223–224 (2003) 301–312

International Journal of Mass Spectrometry

www.elsevier.com/locate/ijms

Limitations in the time resolution of quadrupole mass spectrometry using a flushed extraction probe

J. Laimer*, G. Misslinger, H. Störi

Institut für Allgemeine Physik, Vienna University of Technology, Wiedner Hauptstraße 8-10, A-1040 Wien, Austria

Received 4 March 2002; accepted 13 May 2002

Abstract

At gas pressures higher than approximately 5 mbar it is common practice to use a two-stage pressure reduction set-up to accomplish the needed transition down to the operating pressure of a quadrupole mass spectrometer (QMS). We have demonstrated that, by using a specially constructed helium flushed probe system, a quick transport of species extracted from a process gas to a QMS can be achieved. An experimental investigation using a very fast chemical decomposition process revealed a delay of the signal of more than 50 ms, but a time resolution of only a few milliseconds for this set-up. The broadening of the signal can be explained and described by a combined effect of diffusion during the transport of the species within the probe system and the mean residence time of the species in the ionisation chamber of the QMS. An investigation of the contributions of different effects on the limited time resolution revealed that the present set-up is close to the experimentally possible limits of this technique. However, as an instrument function describing the measurement system was derived with good accuracy, a deconvolution of measurements with the instrument function would allow a time resolution down to 2 ms. (Int J Mass Spectrom 223–224 (2003) 301–312)

Keywords: Mass spectrometry; Gas sampling probe; Time resolution

1. Introduction

Quadrupole mass spectrometers (QMSs) are most widely used for partial pressure measurements. However, due to the geometric dimensions of a QMS and the fact that no gas phase collisions of species should occur within the mass filter and detector of the QMS, the QMS has to be operated at pressures below 10^{-5} mbar [1]. In applications where the process pressure exceeds the normal operation pressure of a QMS, a pressure reduction system is required to accomplish the needed transition. There are already several systems commercially available which are able to perform a defined pressure reduction. For convenience, this transition is often done with a variable leak valve. However, this set-up does not maintain the process gas composition under conditions usually encountered [1]. Process gases with pressures lower than approximately 5 mbar can be easily analysed by extracting gas through a small orifice into a separately pumped QMS [2,3]. The size of the orifice is limited due the fact that molecular flow has to prevail within the orifice and the orifice should not be sensitive to contaminations that could change the conductance. At pressures higher than 5 mbar at least two-stage pressure reduction stages have to be used.

* Corresponding author. E-mail: laimer@iap.tuwien.ac.at

1387-3806/02/$ – see front matter
PII S1387-3806(02)00866-7

Best results can be obtained by doing molecular beam mass spectrometry (MBMS), which makes use of at least two orifices and differential pumping [4–6]. However, due to the two-stage differential pumping the extraction system is rather bulky and cannot be used for all applications. In order to allow a gas extraction with a probe that can be easily inserted into a process to be investigated a two-stage pressure reduction apparatus, consisting of a capillary tube as a first pressure reduction stage and an orifice as a second pressure reduction stage is used [2,7]. Only a fraction of the gas flow through the capillary tube enters the mass spectrometer, most of the gas flows directly to a vacuum pump. Within the capillary tube a viscous flow to a pumped interstage region is maintained where an orifice is located through which the reduced-pressure gas is sampled by molecular flow into the mass spectrometer chamber. However, such a type of set-up does not have a quick response on changes in chemical composition of process gases. In order to reduce the response time, the conductance of the capillary tube has to be increased. However, this also increases the amount of gas extracted from the process under investigation. When the gas flow to be extracted is limited, also the response time is limited. We have demonstrated that, by using a specially constructed helium flushed probe system, a quick transport of species extracted from a process gas to a QMS can be achieved [8–10]. The probe system caused a delay time of a few tens of milliseconds depending on the process pressure and allowed a time resolution of about 23 ms. It turned out that the mean residence time of the extracted process gas within the QMS was the most limiting factor. In order to achieve a better time resolution a careful redesign of the probe and mass spectrometer system was performed and first results were very promising [11].

2. Experimental details

Fig. 1 shows a vacuum schematic of the home-made helium flushed probe system. The principal function of the probe system is to extract gas from a process to be investigated and to transport it quickly to a gas flow splitter, where a portion of this gas is extracted through an orifice to a QMS. Along the probe system a defined pressure reduction has to take place. The probe itself is made of a fused silica capillary and a tube which are melted together in a “U”-shaped form. At the tip of the probe there is a 0.3 mm diameter hole through which the gas from the process gas under investigation is extracted (Fig. 2). High purity (99.9999%) helium (He) is used to flush the probe and transport the

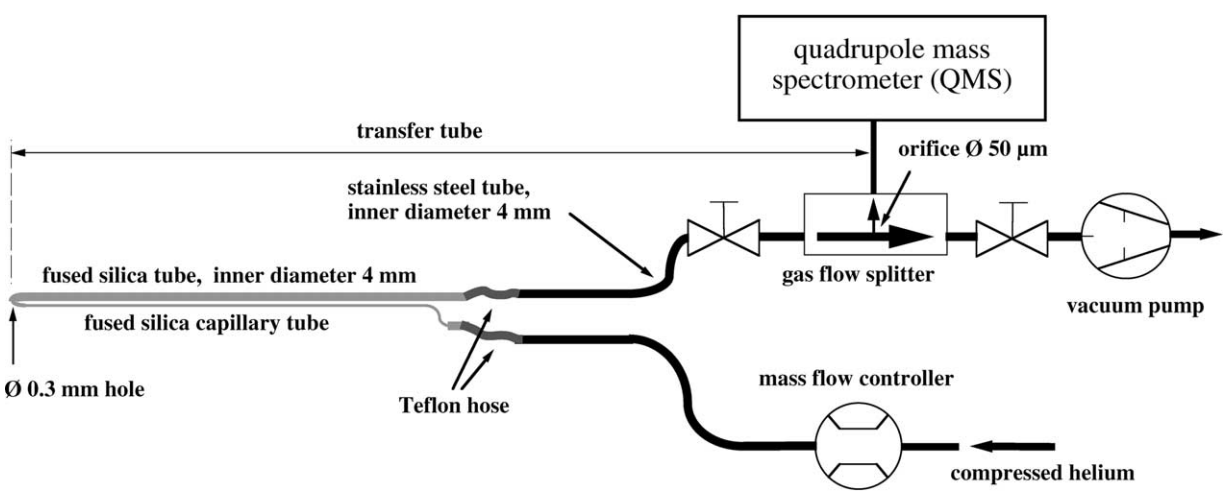

Fig. 1. Schematic illustration of the helium flushed pressure reduction sampling probe.

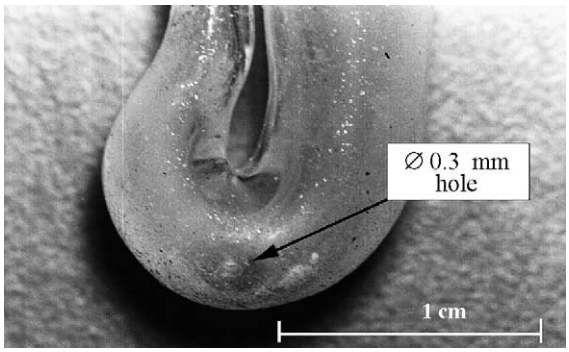

Fig. 2. Photograph of the tip of the sampling probe.

extracted gas to a platinum orifice of 50 μm diameter which is located directly beneath the ion source of the QMS. Helium flow is adjusted in order to extract a gas flow of approximately 10% of the helium flow from the process gas to be analysed. The pressure of the process gas is held constant. From the tip of the probe the gas is guided through a 4 mm inner diameter tube (transfer tube) over a distance of approximately 1.10 m to the mass spectrometer. The gas transport should be accomplished within some 10 ms. A more detailed description of the probe system as well as some properties of the probe system, including pressure distribution, was given in previous papers [8,9]. According to [8], the pressure drop across the entrance hole of the probe system is small. Therefore, the pressure at the beginning of the transfer tube is slightly below the pressure of the process gas under investigation. At the end of the transfer tube the pressure drops down to 2–3 mbar.

Fig. 3 shows a schematic illustration of the vacuum system of the QMS. The QMS is of type QMA 125 from Balzers and is placed in a housing with an additional flange and otherwise unchanged dimensions. The centrepiece of the new experimental set-up is a drilled block of stainless steel, which separates the ionisation chamber from the mass analysis chamber of the QMS. This block contains also the gas flow splitter, which extracts gas from the probe system to the ionisation chamber via a 50 μm diameter platinum orifice. It is designed in such a way that the volume of the ionisation chamber V_1 is as small as possible as well as the conductance to the mass analysis chamber L_{12}. The conductance L_{12} is predominantly caused by the ion source exit orifice, which has a diameter of 2 mm. The volume of the ionisation chamber V_1 is about 0.3 dm^3. The volume of the mass analysis chamber V_2 is about 1.7 dm^3. In order to achieve a short mean residence time of the gas in the ionisation chamber, the ionisation chamber has to be pumped with high pumping speed. The vacuum inside the ionisation chamber is sustained by a turbomolecular pump (type TPU 240 from Balzers) with a pumping speed $S_1 = 230$ L/s (specified for N_2). The vacuum inside the mass analysis chamber is sustained by a turbomolecular pump (type TPU 062 from Balzers) with a pumping speed of $S_2 = 56$ L/s (specified for N_2). Because of the low compression ratio of turbomolecular pumps for light gases a combination of a spiromolecular pump (type MDP 5010 from Alcatel) and a two-stage rotary vane pump (type 2015 from Alcatel) is used as a backing pump system for both turbomolecular pumps.

In order to experimentally characterise the probe and mass spectrometer system, a plasma process with a very fast decomposition of chemical species was used [10,12–14]. As the plasma reactor used is described in detail elsewhere [9,15,16] only a brief description will be given. The reactor basically consists of a 1.2 m long fused silica tube with an inner diameter of 25 mm and with external ring electrodes allowing an electrodeless r.f. discharge (13.56 MHz). The discharge can be operated in a pulsed mode. The reactor is positioned within a furnace allowing a heating of the process gas up to temperatures of 1200 °C. The feed stock consisted of hydrogen (H_2, purity 99.999%) and dichloromethane (CH_2Cl_2, purity 99.9%). The flow rates of all process gases were controlled by mass flow controllers. Process pressures ranging from 20 to 100 mbar were achieved by a rotary vane pump, controlled by a throttle valve and measured by a diaphragm-type gauge. The decomposition experiments have been performed with a process gas mixture of 1% dichloromethane in hydrogen at 20 mbar. For these experiments a furnace temperature of 600 °C and a pulsed discharge with an r.f. peak power of 800 W at a very low pulse

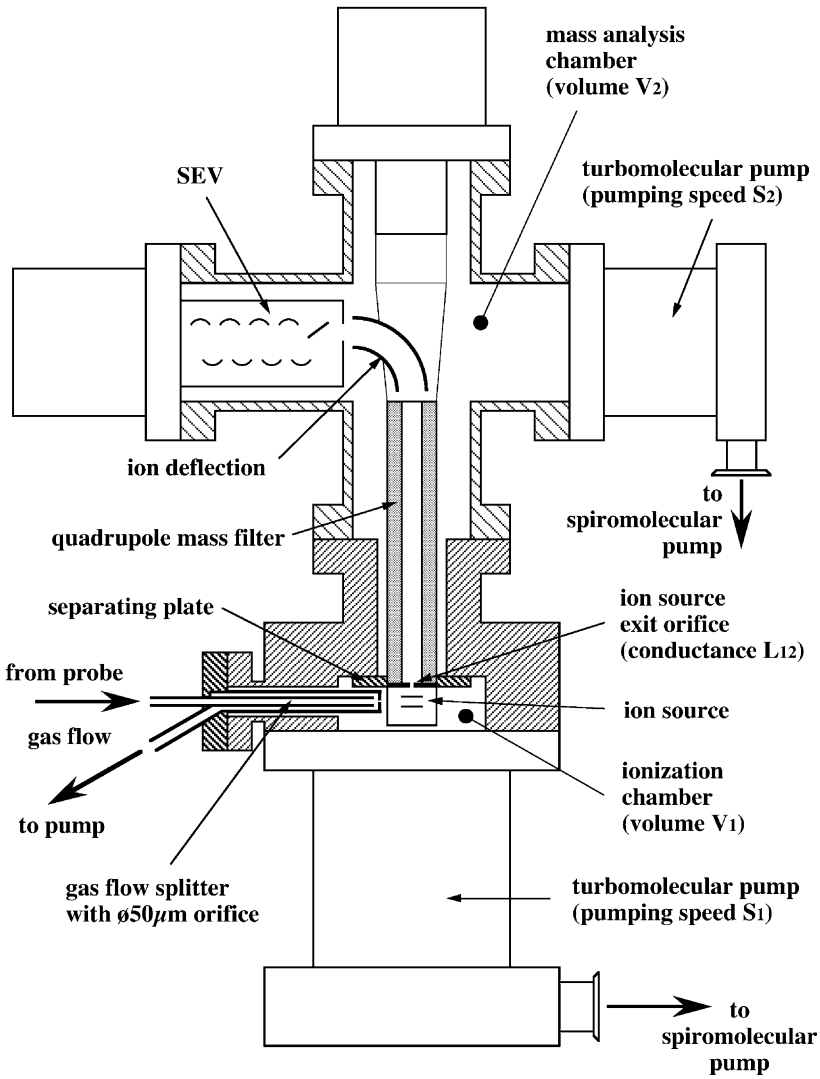

Fig. 3. Schematic illustration of the vacuum system of the QMS.

repetition rate were used. The pulse duration was 300 ms and the pulse pause was 2 s. The probe system was placed in such a way that the tip of the probe system reaches right into the plasma zone. The mass spectrometric measurements were triggered with the rising edge of the r.f. pulse. Therefore, the zero point of the time scale of our measurements corresponds to the plasma switching 'on'. The species being monitored is CH_2Cl_2, one of the feedstock gases, which is rapidly decomposed by the plasma.

3. Theory and comparison with experimental results

Fig. 4 shows a schematic diagram of the vacuum system of the entire measurement set-up. As the time resolution of our previous system was dominated by the mass spectrometer (mean residence time of the gas in the mass spectrometer chamber) and the extraction probe contributed only a delay to the signal, we will start with the mass spectrometer system.

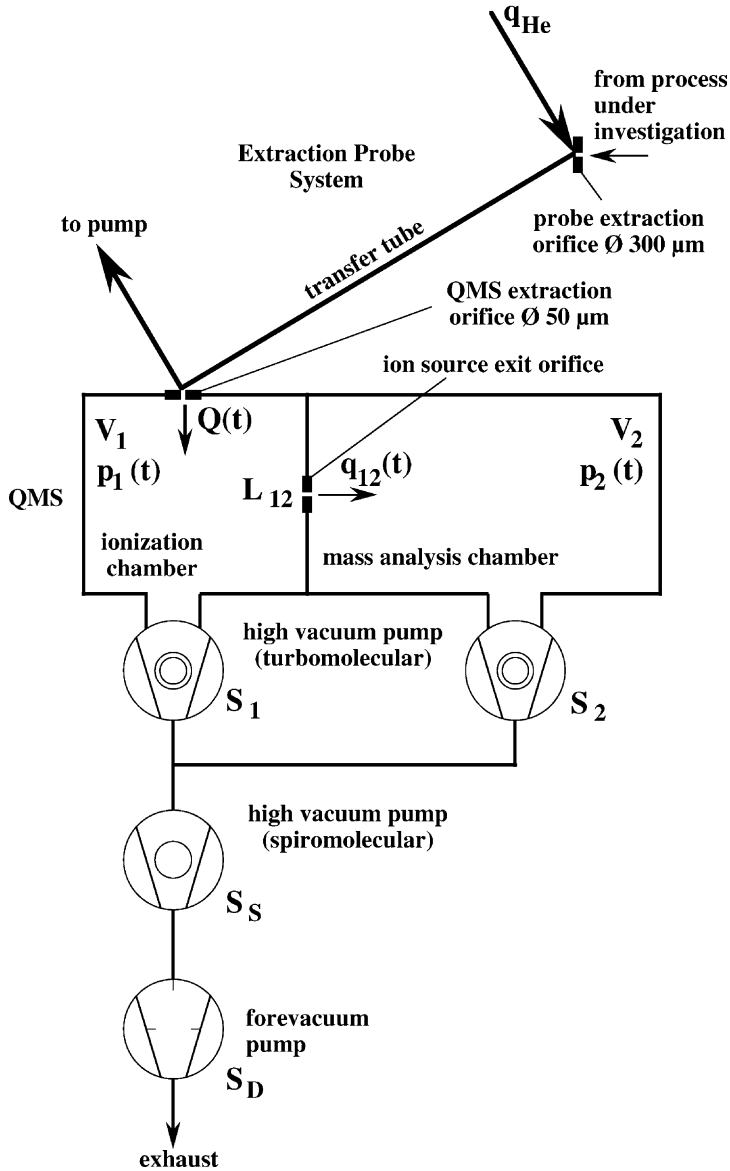

Fig. 4. Schematic diagram of the vacuum system of the extraction probe and QMS.

3.1. Mass spectrometer system

In the present case, we have divided the volume of the mass spectrometer into two parts, which are connected to each other through a small hole (ion source exit orifice). Both parts are separately pumped. In such a case, the mass balance in the mass spectrometer system has to be described with two weakly coupled differential equations of the following form

$$V_1 \frac{\mathrm{d}p_1(t)}{\mathrm{d}t} = Q(t) - p_1(t)S_{1,\mathrm{eff}} - q_{12}(t) \quad (1)$$

$$V_2 \frac{\mathrm{d}p_2(t)}{\mathrm{d}t} = -p_2(t)S_{2,\mathrm{eff}} + q_{12}(t) \quad (2)$$

where

$$q_{12}(t) = (p_1(t) - p_2(t))L_{12} \tag{3}$$

$Q(t)$ denotes the gas flow of species into the ionisation chamber, q_{12} the gas flow between the two chambers of the mass spectrometer, V_1 and V_2 the volumes of the ionisation and mass analysis chamber, respectively, $p_1(t)$ and $p_2(t)$ the time-dependent partial pressures of the species under consideration in the ionisation and the mass analysis chamber, respectively, $S_{1,\mathrm{eff}}$ and $S_{2,\mathrm{eff}}$ the effective pumping speeds at the ionisation and mass analysis chamber, respectively and L_{12} the conductance of the ion source exit orifice. If, for simplicity, the incoming gas flow $Q(t)$ has the form of the scaled Heaviside step function $\Theta(-t)$, which means that

$$Q(t) = Q_0, \qquad t < 0 \tag{4}$$

$$Q(t) = 0, \qquad t > 0 \tag{5}$$

than the following partial pressures for the related species should be caused in the two chambers of the mass spectrometer for $t > 0$

$$p_1(t) = c_1\,\mathrm{e}^{-t/\tau_1} + d_1\,\mathrm{e}^{-t/\tau_2} \tag{6}$$

$$p_2(t) = c_2\,\mathrm{e}^{-t/\tau_1} + d_2\,\mathrm{e}^{-t/\tau_2} \tag{7}$$

where τ_1, τ_2, c_1, c_2, d_1, d_2 are functions of Q_0, V_1, V_2, $S_{1,\mathrm{eff}}$, $S_{2,\mathrm{eff}}$, L_{12}. More details may be found elsewhere [17]. As we are mainly interested in the temporal evolution of the partial pressure in the ionisation chamber (signal to be detected), we need values for τ_1, τ_2, c_1, d_1. In case of helium, a calculation gives $\tau_1 \approx 2$ ms, $\tau_2 \approx 38$ ms and $|c_1/d_1| \approx 4000$. Therefore, within a dynamic range considerably smaller than 4000:1, the development of the partial pressure in the ionisation chamber is dominated by the first term in Eq. (6) and can be approximated by

$$p_1(t) \approx c_1\,\mathrm{e}^{-t/\tau_1} \tag{8}$$

where

$$c_1 \approx \frac{Q_0}{S_{1,\mathrm{eff}}} \tag{9}$$

$$\tau_1 \approx \frac{V_1}{S_{1,\mathrm{eff}}} \tag{10}$$

τ_1 denotes the mean residence time (relaxation time) of species in the ionisation chamber. When the gas flow through the ion source exit orifice is low ($L_{12} \ll S_{1,\mathrm{eff}}$), as in our case, then the time resolution of the mass spectrometer is basically determined by the volume of the ionisation chamber divided by the effective pumping speed at the ionisation chamber. Due to geometric restrictions, the effective pumping speed at the ionisation chamber $S_{1,\mathrm{eff}}$ is smaller than the pumping speed of the turbomolecular pump S_1. As a response to the above described Heaviside step function of the dichloromethane gas flow, we should expect an exponential decrease of the dichloromethane signal of the mass spectrometer in our experiments with a relaxation time equal to the mean residence time of the species in the ionisation chamber.

Fig. 5 shows the experimental result of the decomposition of dichloromethane. In order to compare it with a Heaviside step function the signal is normalised. Also an estimated value of the delay is subtracted from the time scale. As can be seen the dichloromethane signal exhibits first a relatively slow decrease, followed by a steep decrease and finally by an exponential relaxation. The tail of the dichloromethane signal can be described by an exponential relaxation with a relaxation time of ≈2 ms (best fit of the tail of the signal). However, the slow onset of the decomposition cannot be described by a relaxation as can be seen by fits with longer relaxation times in Fig. 5. From the model described before, we can interpret the relaxation time as the mean residence time of the dichloromethane in the ionisation chamber. The deviation of the observed dichloromethane signal from the exponential one is most likely due to effects in the extraction probe system. Therefore, we have to look into this matter in more detail.

3.2. Extraction probe system

The time behaviour of the previous extraction probe system was well described by a plug flow model for the transport of the gas through the tube, causing only a

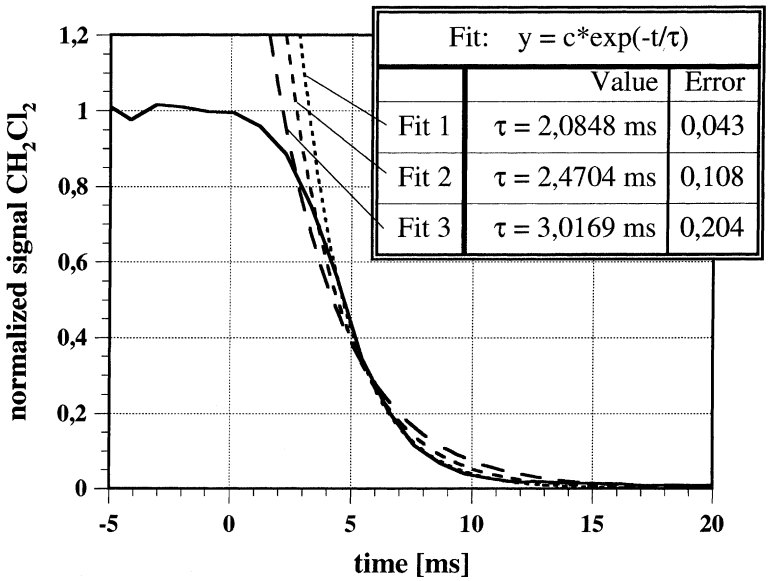

Fig. 5. Experimentally observed time resolved decomposition of dichloromethane. An estimated value of the delay is subtracted from the time scale. The tail of the signal may be fitted with an exponential function. Interval of the normalised signal used for fitting: Fit 1 is 0.6 down to 0.01, Fit 2 is 0.8 down to 0.01, and Fit 3 is 0.9 down to 0.01.

delay of the signal [8]. This description was sufficient as the effects of the extraction probe were negligible compared to a relaxation time in the order of 20 ms. Apparently with shorter relaxation time, effects taking place in the extraction probe have to be taken into account.

The extraction probe consists of three parts contributing to the pressure reduction, the hole in the capillary tube, the transfer tube and the orifice to the mass spectrometer system. As the extracted gas remains during extraction most of the time within the transfer tube, effects within the transfer tube are most likely responsible for the observed deviation of the signal from an exponential relaxation.

A first step would be to include in the above-mentioned plug flow model also diffusion (one-dimensional case). From theory [1], we can easily derive that in such a case a signal (number of molecules of the species under investigation per unit volume) of the form of a scaled Dirac delta function $\delta(z)$ entering the transfer tube

$$n(z, t = 0) = n_0\delta(z) \tag{11}$$

causes a signal along the transfer tube of the form of a Gaussian function

$$n(z, t) = n_0 \frac{1}{\sqrt{4\pi Dt}} \exp\left(-\frac{(z - vt)^2}{4Dt}\right) \tag{12}$$

where z denotes the distance from the entrance of the transfer tube, v the velocity within the transfer tube and D is the diffusion coefficient of the species under investigation in helium (extracted gas is diluted in helium). Thus, a slowly broadening Gaussian profile is propagating along the transfer tube with the gas flow. As the partial pressure of the species $p(z, t)$ is directly proportional to $n(z, t)$ [1], the distribution of the partial pressure is a Gaussian function as well.

However, in our case the incoming signal has the form of the scaled Heaviside step function $\Theta(z)$, which means that

$$n(z, t = 0) = n_0\Theta(z) = n_0 \int_{-\infty}^{z} \delta(z)\, \mathrm{d}z \tag{13}$$

In this case a spatio-temporal distribution of the form of a slightly modified error function $n(z, t)$ is present

within the transfer tube.

$$n(z,t) = n_0 \frac{1}{\sqrt{4\pi Dt}} \int_{-\infty}^{z} \exp\left(-\frac{(z-vt)^2}{4Dt}\right) \mathrm{d}z \tag{14}$$

This function not only describes the signal along the transfer tube at a fixed time t, but also the temporal evolution of the signal at a fixed position z, e.g., at the end of the transfer tube. Please note that, while the spatial distribution at any time t corresponds to a properly scaled error function, the temporal evolution at any fixed position z, which is practically more relevant, corresponds to a slightly distorted properly scaled complementary error function. However, at any position z sufficiently far downstream of the injection, the deviation between a complementary error function and the slightly modified version (Eq. (14)) is for all practical purposes negligible. But is that really an adequate approximation of the signal form at the orifice to the mass spectrometer? We are extracting gas through the walls and not from the centre of the transfer tube. Maybe the signal form is different between centre and wall. In order to answer this question, we performed a two-dimensional simulation. For the calculation of the particle flux density $g(r, z, t)$ within the transfer tube convection as well as diffusion have to be taken into account. Therefore, we may write

$$\vec{g}(r,z,t) = -D\vec{\nabla}n(r,z,t) + v(r)n(r,z,t)\vec{e}_z \tag{15}$$

where $n(r, z, t)$ denotes the particle density depending on axial position z, radial position r and time t, $v(r)$ the velocity depending on radial position r and $\vec{e}_z$ the unit vector in direction of the tube axis. As under our conditions, viscous laminar flow prevails within the transfer tube a parabolic flow profile will develop. Using such a flow profile

$$v(r) = v_0\left(1 - \frac{r^2}{R^2}\right) = 2\bar{v}\left(1 - \frac{r^2}{R^2}\right) \tag{16}$$

where R denotes the inner radius of the tube, v_0 the velocity in the centre and $\bar{v}$ the mean velocity, and the continuity equation

$$\frac{\partial n(r,z,t)}{\partial t} + \vec{\nabla}g(r,z,t) = 0 \tag{17}$$

delivers the following equation in cylindrical coordinates

$$\frac{\partial n(r,z,t)}{\partial t} = D\left(\frac{\partial^2 n}{\partial r^2} + \frac{1}{r}\frac{\partial n}{\partial r} + \frac{\partial^2 n}{\partial z^2}\right) - 2\bar{v}\left(1 - \frac{r^2}{R^2}\right)\frac{\partial n}{\partial z} \tag{18}$$

We solved this equation numerically for the following boundary condition

$$g_r(r = R, z, t) = 0 \tag{19}$$

and the following initial condition

$$n(r,z,t) = n_0\Theta(z) \tag{20}$$

Unfortunately, an investigation of various partial differential equation (PDE) solvers available inside scientific software packages showed that none are able to solve the special form of PDE describing our situation. Our PDE contains a first temporal derivative combined with first and second spatial derivatives. Therefore, a simple difference scheme with hard coded boundary and initial conditions was implemented in a FORTRAN program in order to perform the necessary simulations. The parabolic profile of longitudinal flow velocity was hard coded as well. A two-dimensional grid of typically 10–50 radial and 50–500 longitudinal points was used over 50,000–300,000 time steps. The time step was limited to values where neither diffusion nor flow would transport material by more than one grid cell in either direction. To economise on grid size, the average flow velocity was subtracted from the parabolic velocity profile, essentially immobilising the signal investigated in one area of the computational grid. The code was extensively tested with simulation of pure diffusion and plug flow to verify conformance to analytical solutions, where these are available. Furthermore, after each time step the total amount of material present was computed, giving essentially a constant. This verifies the sanity of the differencing scheme and the influence of rounding errors. Finally, the size of the grid cells and the time step was varied to establish the granularity required. One run of the program took from a few seconds to 1 or 2 min on a

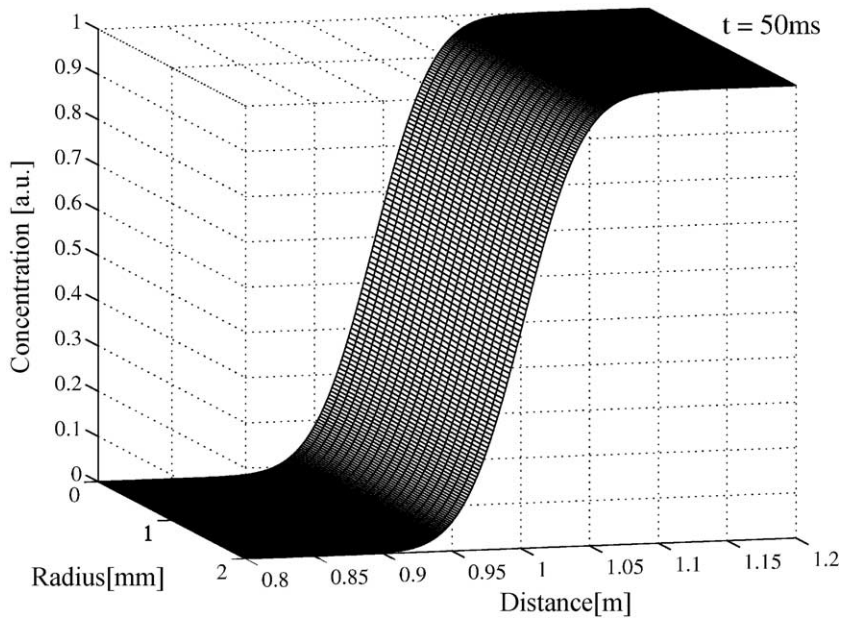

Fig. 6. Result of a numerical simulation of the transport of species within the transfer tube of the extraction probe system. A concentration profile of the form of a Heaviside step function develops after $t = 50$ ms to the shown spatial concentration distribution.

COMPAQ ALPHA-Server DS10, running openVMS, depending on grid size and number of time steps.

Fig. 6 shows the result of the simulation for a simplified condition (average pressure of 10 mbar, diffusion coefficient $D = 0.006\,\mathrm{m^2/s}$ and mean velocity $\bar{v} = 20\,\mathrm{m/s}$). As can be seen, the radial diffusion in our case is so fast that the observed signal is almost independent of the radial position. The signal at the wall has the same profile as in the centre and shows only a delay of <0.1 ms. As the sampling hole at the tip of the probe is even smaller than the radius of the transfer tube, we make the assumption that the signal entering the transfer tube is a step function (Eq. (13)). Therefore, there is no need to allow any time spread in the species concentration at the entrance of the transfer tube. Additionally, the signal form obtained from the numerical simulation looks very similar to an error function. However, compared to the one-dimensional case, the diffusion seems to be enhanced by a factor of 2, assuming $v = \bar{v}$ in Eq. (14). A comparison of this signal form with the results presented in Fig. 5 clearly indicates that the slow onset of the decomposition of the dichloromethane signal in our experiments might be well explained by the diffusion of the extracted species within the transfer tube. Therefore, we may conclude that the temporal response of the transfer tube to a signal of the form of the Heaviside step function $\Theta(z)$ is basically a complementary error function.

3.3. Combined system

In order to describe the combined system, we have to convolute the response function of the extraction probe system (transfer tube) $f_{\mathrm{EP}}(t)$ with that of the mass spectrometer system (ionisation chamber) $f_{\mathrm{MS}}(t)$ as shown below

$$f_{\mathrm{Sys}}(t) = f_{\mathrm{EP}} \otimes f_{\mathrm{MS}} = \int_{-\infty}^{+\infty} f_{\mathrm{EP}}(\tau)\, f_{\mathrm{MS}}(t-\tau)\, \mathrm{d}\tau \tag{21}$$

The instrument function $f_{\mathrm{Sys}}(t)$ is basically the response of the combined measurement system to a Dirac delta function. From chapter 3.2, we know that

the instrument function of the extraction probe $f_{EP}(t)$ may be approximated with a Gaussian function like

$$f_{EP}(t) = \frac{1}{\sqrt{2\pi}\sigma} e^{-(t-t_{D,EP})^2/2\sigma^2} \quad (22)$$

where $t_{D,EP}$ denotes the delay time in the transfer tube and σ the standard deviation describing the broadening of the signal. For practical applications the full width at half maximum ($FWHM_{EP}$) of the signal is better suited, whereby

$$FWHM_{EP} = 2\sqrt{2\ln 2}\sigma \quad (23)$$

From chapter 3.1, we know that the instrument function of the mass spectrometer system $f_{MS}(t)$ may be described with an exponential function like

$$f_{MS}(t) = \frac{\Theta(t)}{\tau_1} e^{-(t/\tau_1)} \quad (24)$$

In order to use the instrument function of the combined system $f_{Sys}(t)$ for a comparison with the measurements, we have first to convolute the instrument function with the expected signal from the decomposition of CH_2Cl_2, which may be approximated with a Heaviside unit function $\Theta(-t)$. The decomposition of CH_2Cl_2 in the plasma proceeds so fast that there is no need to allow any time spread in the species concentration. The used approximation is also supported by experimental measurements performed with increasing r.f. power, as they showed no further reduction in the width of the monitored CH_2Cl_2 signal at power levels above 500 W. The experimental results used for the comparison with the simulation were obtained at an r.f. power of 800 W, which is well beyond this limit.

The function resulting from this convolution was used for a least-square fit to the measurements. A comparison with the experimental result exhibited in Fig. 7 shows an excellent reproduction by the simulation (fitting) indicating that all relevant effects have been included in our simulation. As a result of the fitting, we obtain the following values for the fit parameters: $t_{D,EP} = 52$ ms, $\sigma = 1.5$ ms and $\tau_1 = 1.9$ ms. This gives $FWHM_{EP} = 3.5$ ms. There is only one small discrepancy between the experimental result and the simulation at the far end of the tail. The simulated signal goes faster down to zero. There are several reasons for the small remaining experimental signal still observed. First, we have approximated the instrument function of the mass spectrometer system with only

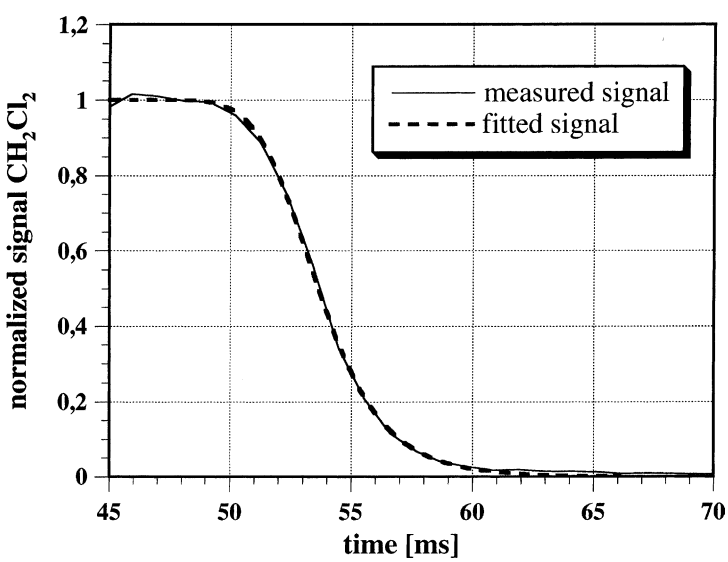

Fig. 7. Comparison of the simulated (fitted) signal with the experimental measurement signal obtained by the QMS.

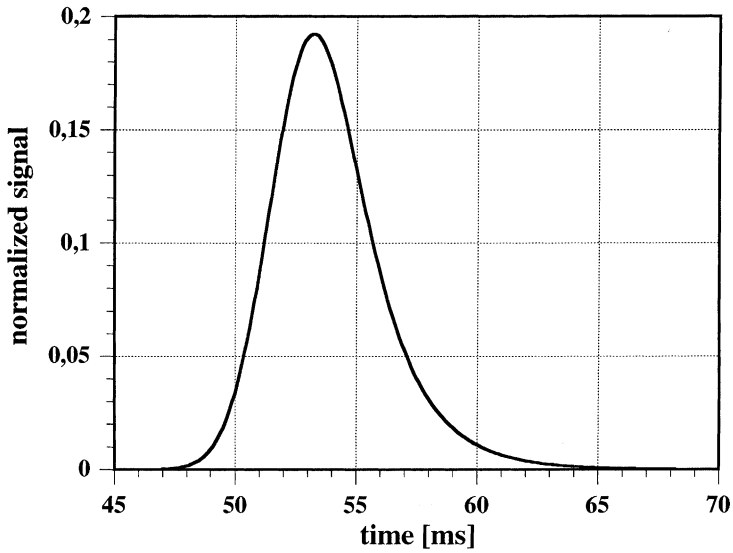

Fig. 8. Determined instrument function of the combined extraction probe and mass spectrometer system.

one exponential function with a time constant of $\tau_1 = 1.9$ ms. From our analysis in chapter 3.1, we know that there should be a small contribution of an additional exponential function with a time constant of $\tau_2 \approx 38$ ms. Furthermore, the model does not account for sticking of molecules to the walls and retention of gas in parasitic volumes. Finally, there is also a minute contribution by noise.

From this finding, we are able to determine the instrument function of our combined system (Eq. (21)), which is shown in Fig. 8. It is basically also the negative first derivative of the smoothed measured signal in Fig. 7. As can be seen, the instrument function may be approximated for all practical purposes with a convolution of a Gaussian function with an exponential function. The instrument function of the combined system shows a delay time of approximately 53.2 ms and a $FWHM_{EP}$ of approximately 4.6 ms.

When one investigates time-resolved decomposition processes using the above described combined system, the "true" temporal evolution of the species cannot be observed by the mass spectrometer. The measured signal is a convolution of the "true" signal with the instrument function of the combined system. However, knowing the instrument function of the combined system allows the determination of the "true" signal from the measured signal by deconvolution. The better the instrument function is known and the lower the noise in the data is, the better the deconvolution can be performed. By doing so, the temporal evolution of gas phase species may be investigated with time resolutions down to approximately 2 ms. Even for nearly perfect data the time resolution, which can be achieved by deconvolution, is unfortunately restricted by the Gaussian component in the instrument function f_{Sys} (Eq. (21)). The Fourier transform of the Gaussian is again a Gaussian, which falls off very steeply to the high frequency end of the spectrum. Thus, information on changes much faster than the half width of the Gaussian is essentially wiped out [18].

4. Conclusions

It has been demonstrated that the developed gas extraction and mass spectrometer system itself allows time-resolved process gas measurements with a time

resolution of a few milliseconds. The time resolution is restricted due to diffusion within the sampling probe as well as due to the mean residence time in the ionisation chamber of the mass spectrometer. A further improvement of the experimental set-up seems to be difficult. Reducing the length of the transfer tube of the sampling probe would reduce diffusion effects, but it would reduce the flexibility of the set-up as well. Therefore, this would only be a possibility for certain applications. Another possibility would be to use another gas for flushing the sampling probe. Diffusion effects would be reduced, when the extracted gas would have a lower diffusion coefficient in the flush gas. However, the number of inert flush gases available with high purity is rather restricted. Also a further reduction of the mean residence time of gas in the ionisation chamber below 2 ms is not easy to accomplish. A further reduction of the ionisation chamber would be possible, but by doing so the effective pumping speed would be reduced as well. Therefore, we believe that the present set-up is close to the experimentally possible limits of this technique.

However, as the effects contributing to the broadening of the signal within the measurement system are well understood and experimentally verified by a measurement on a very fast decomposition process, an instrument function describing the measurement system was derived with good accuracy. A deconvolution of the measurements obtained by the described set-up with the instrument function allows a time resolution down to 2 ms.

The whole analysis presented is based on the assumption that molecules do not stick to the walls of the transfer tube. If they do stick, a description of the system similar to a gas chromatograph would be more adequate, yielding a transfer time and signal broadening orders of magnitude larger [19]. In such situations an inert inside coating of the tube could be envisaged.

Acknowledgements

The authors gratefully acknowledge financial support of the present work by the Austrian Science Foundation FWF under Project no. P12054.

References

[1] J.M. Lafferty (Ed.), Foundations of Vacuum Science and Technology, Wiley, New York, 1998.
[2] Vacuum Technology 2002, Pfeiffer Vacuum GmbH, Emmeliusstrasse 33, D-35614 Asslar, Germany.
[3] Hiden HPR-30 Series Process Gas Analysers, Hiden Analytical Ltd., 420 Europa Boulevard, Warrington WA5 5UN, England.
[4] HPR-60 Molecular Beam Radicals & Neutrals Measurement System, Hiden Analytical Ltd., 420 Europa Boulevard, Warrington WA5 5UN, England.
[5] C. Rego, R.S. Tsang, P.W. May, M.N.R. Ashfold, K.N. Rosser, J. Appl. Phys. 79 (1996) 7264.
[6] J.R. Petherbridge, P.W. May, S.R.J. Pearce, K.N. Rosser, M.N.R. Ashfold, J. Appl. Phys. 89 (2001) 1484.
[7] Hiden HPR-20 Series Precission Gas Analysis System, Hiden Analytical Ltd., 420 Europa Boulevard, Warrington WA5 5UN, England.
[8] J. Laimer, O. Schnabl, C.G. Schwärzler, H. Störi, J. Vac. Sci. Technol. A 14 (1996) 2315.
[9] C.G. Schwärzler, O. Schnabl, J. Laimer, H. Störi, Plasma Chem. Plasma Process 116 (1996) 173.
[10] G. Misslinger, J. Laimer, H. Störi, in: M. Hrabovsky, M. Konrad, V. Kopecky (Eds.), Proceedings of the 14th International Symposium on Plasma Chemistry (ISPC-14), Institute of Plasma Physics, Academy of Science of the Czech Republic, 1999, p. 1703.
[11] J. Laimer, G. Misslinger, H. Störi, Vacuum 61 (2001) 435.
[12] M. Asmann, J. Heberlein, E. Pfender, Diamond Relat. Mater. 8 (1999) 1.
[13] G. Misslinger, J. Laimer, H. Störi, Vacuum 61 (2001) 413.
[14] J. Laimer, G. Misslinger, H. Störi, New Diamond Front. Carbon Technol. 11 (2001) 173.
[15] J. Laimer, R. Posch, G. Misslinger, C.G. Schwärzler, H. Störi, Meas. Sci. Technol. 6 (1995) 1413.
[16] J. Laimer, F. Huber, G. Misslinger, H. Störi, Vacuum 47 (1996) 183.
[17] G. Misslinger, Reaktionskinetik bei der plasmaunterstützten Diamantsynthese, Dissertation, Vienna University of Technology, 2002.
[18] R.N. Bracewell, The Fourier Transform and Its Applications, 2nd Edition, McGraw-Hill, New York, 1986.
[19] C.F. Poole, S.K. Poole, Chromatography Today, Elsevier, Amsterdam, 1991.